Application of displacement behavior on tunnel design

Jeong, Yun-Young, Choi, Hae-Joon (Tunnel Div. Chungsuk Eng. Co., Seoul, Korea)
Lee, Jae-Ho (Kyungpook university, Daegu, Korea)
Bang, Jin-Ho (Tunnel Div. Chungsuk Eng. Co., Seoul, Korea)

1. INTRODUCTION

The stability control under tunnel construction deeply relates on displacement behavior of rock mass, estimation for the final values of displacement convergence after two or three times of tunnel diameter advance. Tunnel design before underground excavation should be based on the assumption of displacement behavior estimated from similar geological condition because of data absence on field measurement at arch crown and surface subsidence. Measurement data gathered during the construction work in many fields has some problems, which the first measurement is usually obtained after a lot of initial displacement of surrounding rock mass occurred, and so displacement development does not contain preliminary displacement before excavation and initial one immediately after excavation. Tunnel survey has generally focused on the estimation of the maximum displacements in tunnel arch and crown as like the estimation studies of final deformation from the initial displacement (Song et al., 2002; Chung et al., 1993).

This paper focused on a rational method about the estimation of displacement behavior on arch crown and tunnel stability in preliminary tunnel design. The method is a hybrid consideration of three parts – the first is displacement development obtained by 3D numerical simulation before and after a cut face reaches to measurement points on arch crown, the second is the maximum displacement from field measurement on tunnel excavation, the third is an assessment of tunnel stability through the critical strain proposed by Sakurai(1981). For application of the above method on preliminary tunnel design, it was selected the section that closed to the base pile of Gimpo airport cargo building and a different shape type was resulted from the direct connection between Inchon international airport railway and subway line 9 without any facilities.

2. PRELIMINARY TUNNEL PLAN

2.1 Tunnel Sections

For tunnel sections of Inchon international airport railway contacting with Seoul subway line 9, there are connection area around station facilities, passing sections under Gimpo airport cargo and variable shape sections with parallel track as line alignment shown in Fig. 1.

Fig. 1 Scheme of tunnel sections

Upper and below tracks of Inchon international railway around Gimpo airport cargo were crossed from weak rock with RQD range of 0 ~ 23 % to hard rock with that of 35 ~ 100 %. This rock mass geologically consisted of granite and gneiss, showed engineering properties as summarized in Table 1 through empirical equations from RMR, laboratory test and field hydraulic jack test. The sections under Gimpo airport cargo located in rock mass of V or IV rating.

Table 1. Rating and Engineering properties of rock mass

Parameters	Rating				
	I	II	III	IV	V
Deformation modulus, E_m (GPa)	53.5	26.2	6.8	2.6	0.9
Poisson' ratio	0.2	0.23	0.25	0.27	0.29
Unit weight (g/cm^3)	2.7	2.6	2.5	2.5	2.4
Cohesion (MPa)	32.2	9.3	6.6	4.5	0.9
Friction angle (°)	45	41	37	35	33

2.2 Shape type and support

For passenger' convenience at transfer between Inchon international railway and subway line 9, tunnel excavation had to be done to cover the level difference of both railways. Upper track and below track had to be passed respectively at different level around Gimpo airport cargo as shown in Fig. 2. Upper track located in the very close distance of the maximum 1.73 m from the base pile of cargo building.

Fig.2 Cross cut of tunnel sections

Therefore, there were some kinds of shape type in cross sections as denoted in Fig. 3. Left figure (a) of Fig. 3 is a typical shape for the stability around the base pile of Gimpo airport cargo building, figure (b) and (c) of that is a shape of variable shape sections which one-track line is translated to double-track lines

at the planned level of Inchon international railway.

Fig. 3 shape type of cross sections

One-track line tunnel passing under Gimpo airport cargo had a horseshoe shape section of width 7.1 m., arch crown of below track was apart only 0.2 m from the left side at invert of upper track lining. From the level difference of the both track and the above closeness between the upper track and pile of cargo building in weak rock, it was thought for ground support around the pile to be needed. Micro silica grouting had firstly performed as injection boundary of 7.0 m, injection depth of 20 m and injection angle of 20°. Arch crown of tunnel was supported before excavation by umbrella method; c.t.c. 500 mm, diameter 800 mm of steel pipe. After the preliminary supports by umbrella method, the tunnel excavation had performed in turn according to the excavation schedule of preliminary supporting on below track, excavation of upper face, rock bolting and shotcrete, excavation of below face, rock bolting and shotcrete, concrete lining on the below track line, and then preliminary supporting on upper track, excavation of upper face, rock bolting and shotcrete, excavation of below face, rock bolting and shotcrete, finally concrete lining on the upper track line as denoted in fig. 4.

Fig 4. Construction flow on one-track line tunnel

Relating to the stability of one-track line tunnel under Gimpo airport cargo, survey work focused on the tunnel deformation during construction.

3. TUNNEL SURVEY

3.1 Survey plan

Tunnel deformation was recently estimated by crown settlements and displacement from tunnel wall at five measurement points on each track as denoted in Fig. 5 during two months. This measurement was performed in the interval of 20 m according to tunnel excavation. Two cross sections under Gimpo airport cargo and that around the cargo were the necessary measurement sections for the stability of tunnel excavation. Weekly measurement was carried out by convergence tape extensometer on the record as denoted in Table 2 about a cross section (22km260) of upper track. Performance criteria in Table 2 was reasonable scale if it was compared with another abroad criteria summarized in Table 3.

Fig. 5 five measurement points on each track in a cross section

Table 2. a sample record of weekly measurement in a cross section (22km260) of upper track

Data		Performance criteria (mm)				Measurement (mm)	
		Stable	Level I (warning)	level II (daily check)		Ex-check	check
Crown settlement	O CS	under 5.23	~ 80	over 80	10mm/day	5.5	5.4
Displacement of tunnel wall	■ D-1	under 4.58	~ 50	over 50	10mm/day	5.7	5.9
	▲ D-2	under 4.58	~ 50	over 50	10mm/day	4.0	4.0
	+ D-3	under 4.58	~ 50	over 50	10mm/day	0.0	0.6
	× D-4	under 4.58	~ 50	over 50	10mm/day	0.0	1.2

Table 3. Another abroad criterion about crown settlements and displacement inward (Chun et al, 1996)

Rock	Deformation modulus, E_m (GPa)	Crown settlement (mm)			Displacement inward (mm)	
		Japanese			Austrian	Japanese
		Level I	Level II	Level III	3~4% of rockbolt length	One track line
Weathered rock	0.15	13.6	44.2	1.29	90.0~120	under 75.0
Weak rock	1.0	5.1	18.7	51.0	90.0~120	under 75.0

3.2 Tunnel deformation

Tunnel deformation could be analyzed by tunnel convergence described as in Fig. 6, which final displacement (D_{final}) of tunnel surface is defined as an equation (1).

$$D_{final} = D_p + C_i + D_m \tag{1}$$

where D_p is displacement until tunnel excavation approached to a cross section, C_i is displacement measured in the cross section on that tunnel excavation advanced to x distance over the section and D_m is displacement measured from C_i to the final displacement.

Fig. 6 Generalized form of tunnel convergence

In preliminary tunnel plan, the final displacement of tunnel surface is the crucial data of tunnel stability and deformation. It relates to the final displacement estimated from the tunnel convergence $C(x)$ measured as the above C_i and D_m that was defined as an exponential equation (1) in elastic model, a

fractional function (2) in elastic-plastic model and a composition function (3) in viscoelastic model by preliminary studies (Moon et al., 2001; Song et al., 2002).

$$C(x) = a\{1 - \exp(-bx)\} \tag{1}$$

$$C(x) = C_x\left\{1 - \left(\frac{X}{X+x}\right)^2\right\} \tag{2}$$

$$C(x,t) = a\{1 - \exp(-bx)\} + c\{1 - \exp(-dt)\} \tag{3}$$

where a, b, c, d are constant, t is time and C_x is C_i at x distance apart from a cross section.

As the above survey plan, survey work of a cross section was performed in two months and then the next section after tunnel excavation advanced at x distance. The maximum displacement of crown settlement and tunnel wall were measured respectively about upper track and below track as summarized in Table 4. And so the displacement of upper track was obtained after rock mass was some loosed by means of below track excavation before upper track excavation. It could be not appropriate for regression analysis about displacement behavior.

Table 4. The maximum displacement of crown settlement and tunnel wall

		Displacement (mm) of below track (sta. 22kmOOO)				Displacement (mm) of upper track (sta. 22kmOOO)			
		280	300	320	340	280	300	320	340
Crown settlement	O CS	- 2.8	- 2.4	- 1.5	- 1.8	- 5.8	- 5.8	- 5.5	- 2.9
Displacement of tunnel wall	■ D-1	1.6	1.3	1.2	1.5	5.5	5.0	4.9	2.3
	▲ D-2	- 1.8	- 1.3	- 2.3	- 1.4	- 4.3	- 4.0	- 3.8	- 1.4
	+ D-3	0.4	0.2	1.2	0.9	2.1	-	-	-
	× D-4	0.4	0.6	1.4	1.2	2.8	-	-	1.9

4. 3D NUMERICAL ANANLYSIS

4.1 Model

Tunnel sections under Gimpo airport cargo had geometrically unusual shape with the different level between upper track and below track as one track line as described in Fig. 5. It was not sufficient to find out the interaction between both tracks that tunnel survey had progressively performed according to

tunnel construction step in the certain period. 3D numerical computation was used for investigating not only the interaction between both tracks, but also the displacement (D_p) on the time that tunnel excavation approached to the measurement points.

Model boundary was defined as the minimum area includes four cross sections used for tunnel survey in chapter 3. Simulation of tunnel excavation and support was executed under the same condition except micro silica grouting around the pile of cargo building as three dimensional model described in Fig. 7.

Fig.7 Three dimensional model boundary

Simulation model had the properties of Mohr –Coulomb model resulted from Heok-Brown parameters. The elastic stiffness of pre-reinforced zones by umbrella grouting (Song and Cho, 2006) and the geological data for ground resulted in the physical properties of Table 5 used as input data of this simulation.

Table 5. Input data of this simulation

Model elements	Deformation modulus E_m (GPa)	Cohesion (MPa)	Friction angle (°)	Unit. Weight (tf/m^3)
Silt	0.04	0.10	30	1.9
Silt + sand	0.43	0.20	32	2.3
Gneiss	0.9	0.90	33	2.4
Granite	2.6	4.5	35	2.5
Reinforced area	0.97	0.91	33	2.4

4.2 Deformation behavior

Tunnel deformation obtained through the above simulation was analyzed as the deformation of crown and tunnel wall in the point of the interaction between two tracks during tunnel construction. Fig.8 shows deformation behavior in the crown (Cp4) of below track at sta. 22km300 and 22km320 beneath the pile of the cargo building. It was found that previous displacement occurred respectively 1.57 mm and 1.60 mm until that tunnel excavation advanced to the cross section of sta. 22km300 and 22km320. Crown settlement rapidly increased before and after tunnel excavation at the cross section, additional excavation of upper track induced the displacement increase of about 0.36 mm before tunnel excavation advanced to the same section of upper track.

Fig. 8 Deformation behavior in Cp4 of below track at sta. 22km300 and 22km320

Fig. 9 shows deformation behavior in the left wall (Cp5) of below track at sta. 22km300 and 22km320. It was found that previous displacement occurred respectively 2.61 mm and 2.09 mm until that tunnel excavation advanced to the cross section of sta. 22km300 and 22km320. Displacement outwards of tunnel surface rapidly increased before and after tunnel excavation at the cross section, additional excavation of upper track induced the displacement increase of about 0.58 mm on that the excavation approached to the same section of upper track.

Fig. 9 Deformation behavior in Cp5 of below track at sta. 22km300 and 22km320

Fig. 10 shows deformation behavior in the right wall (Cp6) of below track at sta. 22km300 and 22km320. It was found that previous displacement occurred respectively 2.97 mm and 2.43 mm until that tunnel excavation advanced to the cross section of sta. 22km300 and 22km320. Displacement inwards of tunnel surface rapidly increased before and after tunnel excavation at the cross section, additional excavation of upper track induced the displacement decrease of about 0.38 mm on that the excavation approached to the same section of upper track.

Fig. 10 Deformation behavior in Cp6 of below track at sta. 22km300 and 22km320

Fig. 11 shows deformation behavior in the crown (Cp1) of upper track at sta. 22km300 and 22km320. It was firstly found that the tunnel excavation of below track until the construction step 54 induced the rock mass around the crown of upper track loosed. After previous displacement of about 1.8 mm was induced, crown settlement occurred respectively 2.75 mm and 2.93 mm until that tunnel excavation advanced to the cross section of sta. 22km300 and 22km320. The settlement rapidly increased before and after tunnel excavation at the cross section, too.

Fig. 11 Deformation behavior in Cp1 of upper track at sta. 22km300 and 22km320

Fig. 12 shows deformation behavior in the left wall (Cp2) of upper track at sta. 22km300 and 22km320. It was found that the tunnel excavation of below track caused only a few of deformation in rock mass around the left wall (Cp2) of upper track. Displacement outwards from tunnel surface occurred respectively 1.22 mm and 1.47 mm until that tunnel excavation advanced to the cross section of sta. 22km300 and 22km320. The displacement rapidly increased before and after tunnel excavation at the cross section, too.

Fig. 12 Deformation behavior in Cp2 of upper track at sta. 22km300 and 22km320

Fig. 13 shows deformation behavior in the right wall (Cp3) of upper track at sta. 22km300 and 22km320. It was firstly found that the tunnel excavation of below track induced some displacement in the rock mass around the right wall of upper track. Displacement inwards from tunnel surface occurred respectively 2.74 mm and 2.77 mm until that tunnel excavation advanced to the cross section of sta. 22km300 and 22km320. The displacement rapidly increased before and after tunnel excavation at the cross section, too.

Fig. 13 Deformation behavior in Cp3 of upper track at sta. 22km300 and 22km320

It was thought that the above simulation result proved the interaction between upper and below track during the tunnel construction. Previous deformation (D_p)in the arch crown and tunnel wall of both tracks was summarized about the cross section of sta. 22km280, sta. 22km300, 22km320 and 22km340 in Table 6.

Table 6. Previous deformation (D_p) in the arch crown and tunnel wall of both tracks

Measurement points		Previous deformation, D_p			
		Sta. 22km280	Sta. 22km300	Sta. 22km320	Sta. 22km340
Upper track	Cp1	- 3.34 mm	- 2.75 mm	- 2.93 mm	- 3.29 mm
	Cp2	1.33 mm	1.22 mm	1.47 mm	2.54 mm
	Cp3	- 2.77 mm	- 2.74 mm	- 2.77mm	- 3.01 mm
Below track	Cp4	- 1.33 mm	- 1.57 mm	- 1.60 mm	- 2.38 mm
	Cp5	2.12 mm	2.61 mm	2.09 mm	2.85 mm
	Cp6	- 1.82 mm	- 2.97 mm	- 2.43 mm	- 3.03 mm

5. TUNNEL DEFORMATION AND STABILITY

5.1 Estimation of the final deformation

Numerical computation suggested the estimation of the previous deformation and three dimensional behaviors between both tracks. The final deformation of tunnel surface induced from numerical solution is usually close to the result of tunnel survey, but it shows some difference because of regional geological condition. In this paper, the final deformation (D_{final}) was defined as an equation (4).

$$D_{final} = D_p + D_{survey} + D_{m'} \quad (4)$$

Where D_p is defined as the same denoted in an equation (1), D_{survey} is the maximum value of the crown settlement and the displacement of tunnel wall resulted from the tunnel survey, $D_{m'}$ is displacement resulted from the interaction between upper and below tracks.

The final deformation of measurement points at both tracks were summarized in Table 7 according to an equation (4).

Table 7. The final deformation of measurement points at both tracks

Measurement points		Final deformation, D_{final}			
		Sta. 22km280	Sta. 22km300	Sta. 22km320	Sta. 22km340
Upper track	Cp1	- 9.14 mm	- 8.55 mm	- 8.43 mm	- 6.19 mm
	Cp2	6.83 mm	6.22 mm	6.37 mm	4.84 mm
	Cp3	- 7.07 mm	- 6.74 mm	- 6.57mm	- 4.41 mm
Below track	Cp4	- 4.49 mm	- 4.32 mm	- 3.46 mm	- 4.54 mm
	Cp5	4.52 mm	4.51 mm	3.86 mm	5.08 mm
	Cp6	- 3.19 mm	- 3.87 mm	- 4.36 mm	- 4.03 mm

5.2 Tunnel stability and critical strain

How the above final deformation is analyzed about the tunnel stability was the theme of this paper. It was, therefore, necessary the method assessing the results of displacement measurements rather than stress behavior in tunnels. The method utilizing the critical strain (Sakurai, 1981; Sakurai, 1997) and apparent Young's modulus estimation was used in this paper.

Apparent Young's modulus means the Young's modulus is defined as equations (5), which calculated from the displacement measurement of tunnel surface during the construction.

$$E_c' = \frac{(1-\nu^2)\cdot a\cdot\omega\cdot H}{U_c'}\left\{2K_o' - \frac{(1-2\nu)}{(1-\nu)}\right\} \quad (5)$$

Where E_c' is apparent Young's modulus about the crown settlement, U_c', U_h' is respectively the measurement value of the crown settlement and displacement from tunnel wall, ω is unit weight, H is overburden height, a is the radius of tunnel, ν is Poisson' ratio and K_o' is initial stress ratio.

K_o' was the ratio relating to initial stress of rock mass, but defined by displacement measurement as an equation (6).

$$K_o' = \frac{2(1-\nu)U_c' + (1-2\nu)U_h'}{2(1-\nu)U_h' + (1-2\nu)U_c'} \tag{6}$$

The critical strain (ε_θ) at the crown settlement was simply defined as the proportion of settlement extent (U_c) to the tunnel radius (a) as an equation (7).

$$\varepsilon_\theta = \frac{U_c}{a} \tag{7}$$

Sakurai recently proposed the relation between the critical strain and apparent Young's modulus as an index described in Fig. 14. The displacement measurements carried out in many cases and the apparent Young's modulus result from the tunnel deformation were described as a point mark included in the division indicated whether the arch crown of tunnel was stable or not stable during the tunnel construction. Some unstable division indicated that the tunnel deformation was generally stable, but a few of cases showed unstable deformation.

Fig. 14 Critical strain and apparent Young' s modulus estimation

The above estimation method was applied about the geological condition around the Gimpo airport cargo, the previous deformation (D_p) induced from three dimensional numerical analysis and the final deformation defined according to an equation (4). Fig. 15 showed the tunnel stability of one-track line sections around the Gimpo airport cargo about the crown settlement for tunneling condition with the final deformation and the parameters respectively summarized in Table 7 and Table 8. It was consequently found that the crown settlement of upper track was in the stable range, but additional support was necessary in the point of tunnel design, and then the deformation extent of below track was more stable than that of upper track. Also, it was considerable as the additional support that micro silica grouting was performed beneath the pile of cargo building.

Table 8 Parameters related to apparent Young' s modulus estimation

Parameters	Data summary
Overburden height (H)	27.7 m
Tunnel radius (a)	4.2 m
Unit. Weight (ω)	2.4 tf/m^3
Poisson's ratio (ν)	0.32
Initial stress ratio (K_o')	1.2

Fig. 15 Critical strain and apparent Young s modulus estimation about tunneling around the airport cargo

6. CONCLUSION

In tunnel sections of Inchon international airport railway contacting with Seoul subway line 9, tunnel survey has been recently performed during the tunnel construction. The section around the Gimpo airport cargo was one track parallel line with the level difference between upper and below tracks, the crown displacement and the displacement in tunnel wall was measured during about two months according to the construction steps. The result of displacement measurements was not clear to find the previous deformation (D_p) and the interaction between both tracks, which they were supported by numerical simulation of three dimensional modeling. The final deformation of tunnel section was estimated in this paper by the previous deformation, the maximum displacement during tunnel survey and the interaction between both tracks.

As the last step of tunnel stability analysis, the critical strain and apparent Young's modulus estimation was carried out. It was consequently found that the crown settlement of upper track was in the stable range, but additional support was necessary in the point of tunnel design, and then the deformation extent of below track was more stable than that of upper track. Also, it was considerable as the additional support that micro silica grouting was performed beneath the pile of cargo building.

Finally, if there were database of similar geological condition for replacing with the above tunnel survey, it was thought that the above analysis of tunnel stability could be used in preliminary tunnel plan.

REFERENCE

1. Chung, H.J., K.T. Cho, T.Y. Kim and Y.I. Kim, 1993, A case study on displacement forecasting

method in tunneling by NATM in urban area, Proc. KGS Spring 93 National Conference, Seoul, 27-32.

2. Chun, B.S., M.G. Lee, S.S. Nam and G.S. Shin, 1996, A case study on the displacement behavior of the subway NATM, Proc. KGS Spring 93 National Conference, Seoul, 183-204.
3. Moon, S.B., S.G. Song, H.S. Yang, Y.S. Jeon and G.C. Han, 2001, A numerical analysis study for the prediction of convergences and characteristic of subsidence behavior in shallow, wide tunnel excavation, Tunnel & Underground, Vol. 11, 20-29.
4. Sakurai, S., 1981, Direct strain evaluation technique in construction of underground openings, Proc. 22nd US Symp. Rock Mech., Cambridge, Massachusetts, M.I.T., 278-282.
5. Sakurai, S., 1997, Lessons learned from field measurements in tunneling, Tunnelling and Underground Space Technology, Vol. 12, 453-460.
6. Song, S.G., H.S. Yang, S.S. Lim and S.K. Chung, 2002, Estimation of final deformation of hard rock tunnel using early measured deformation, Tunnel & Underground, Vol. 12, 99-106.
7. Song, K.I. and G.C. Cho, 2006, Equivalent design parameter determination for effective numerical modeling of pre-reinforced zones in tunnel, Tunnelling Technology, Vol. 8, 151-163.

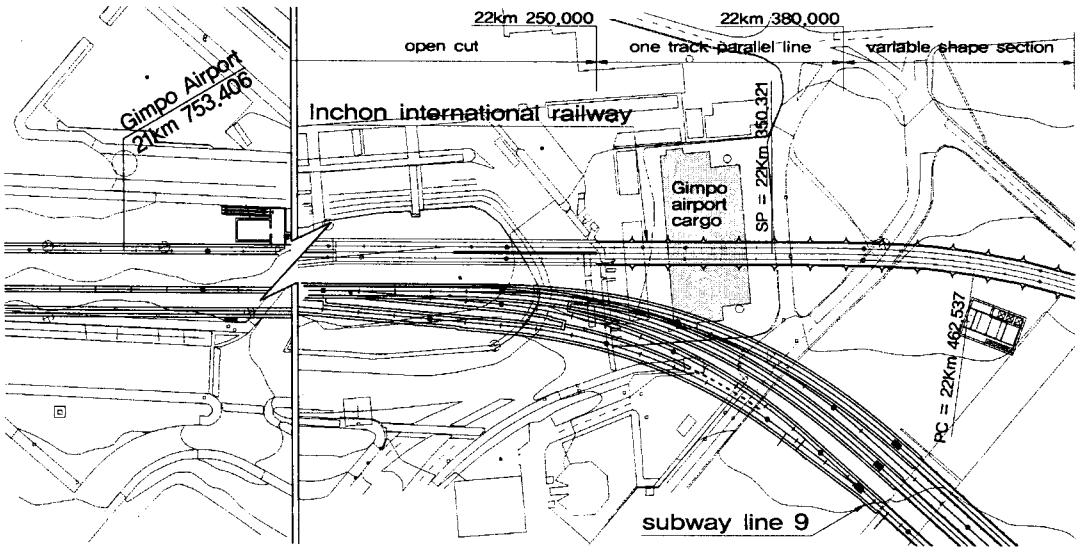

Fig. 1 Scheme of tunnel sections

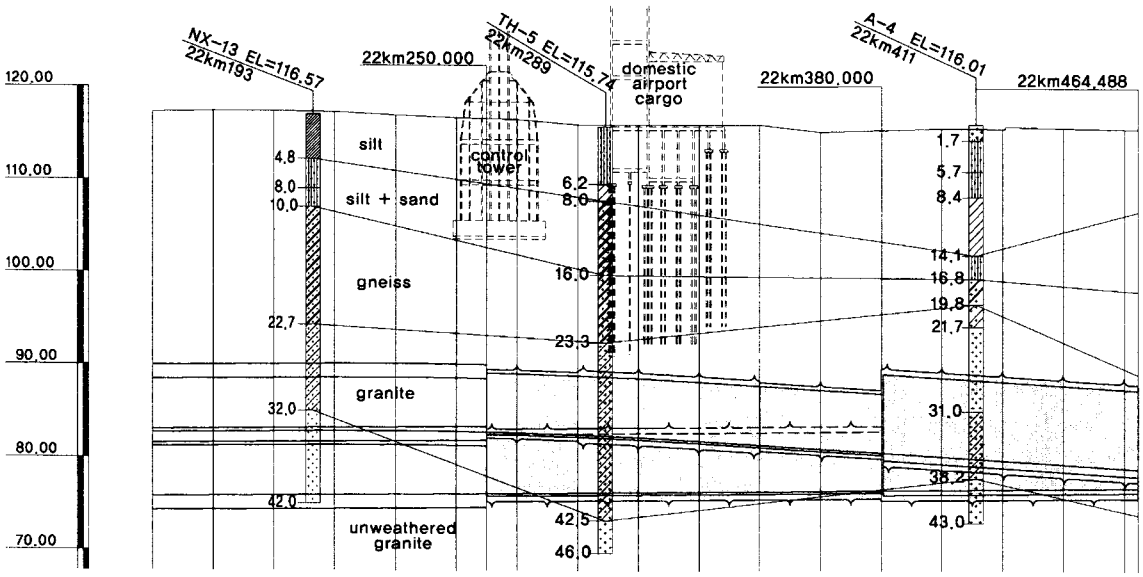

Fig.2 Cross cut of tunnel sections

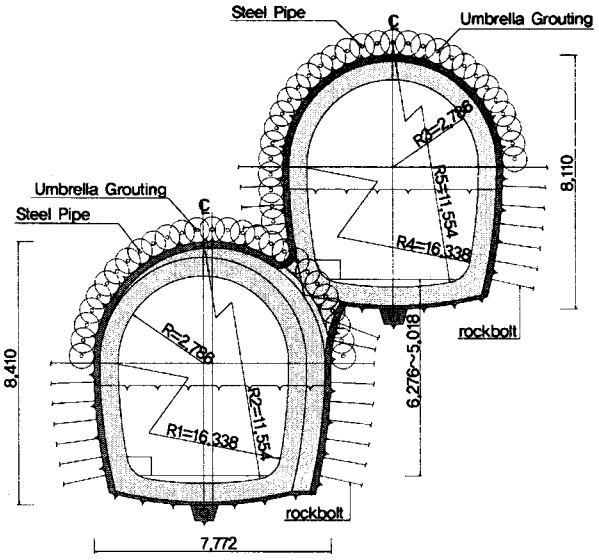

(a) A typical shape

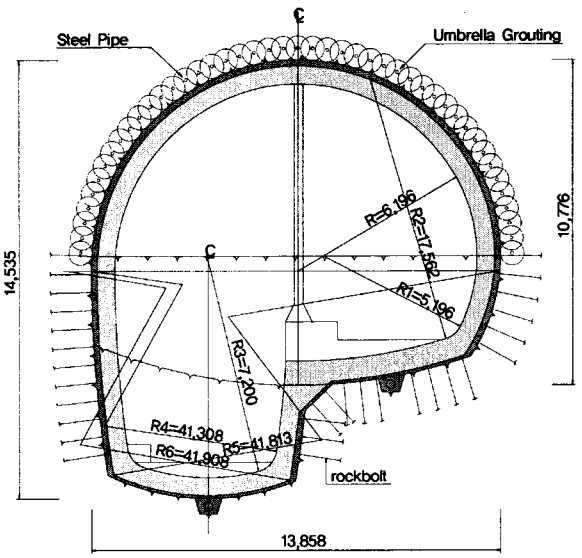

(b) A shape of variable shape section I

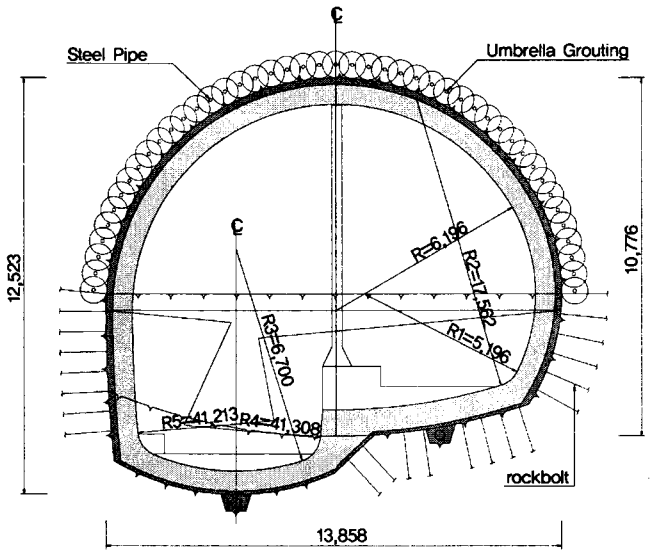

(c) A shape of variable shape section II

Fig. 3 shape type of cross sections

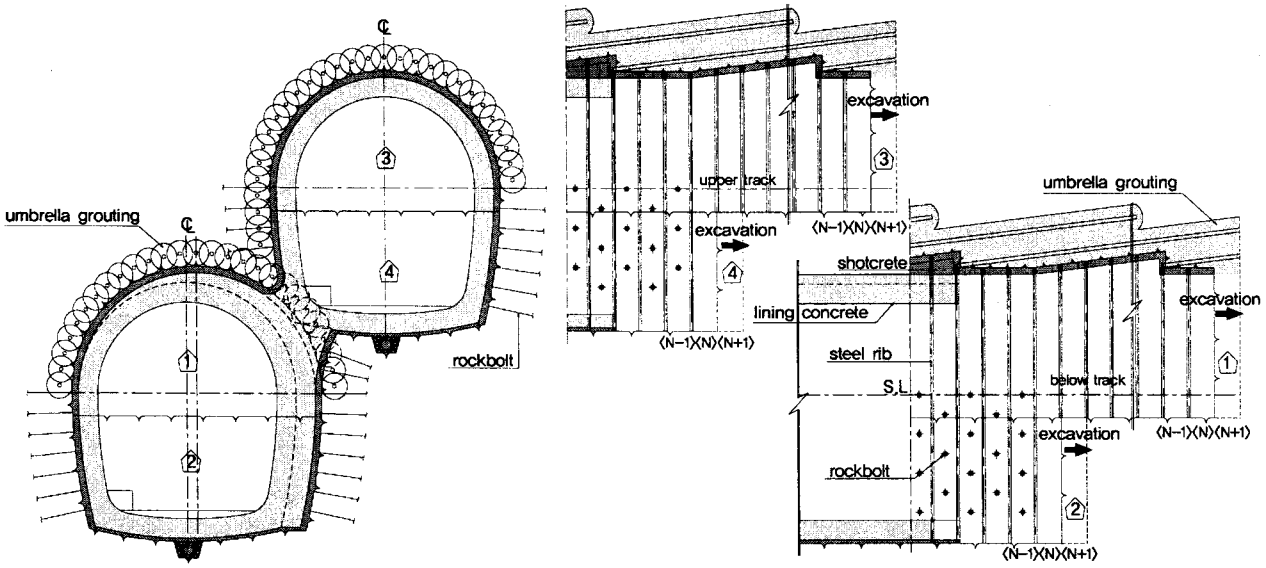

Fig 4. Construction flow on one-track line tunnel

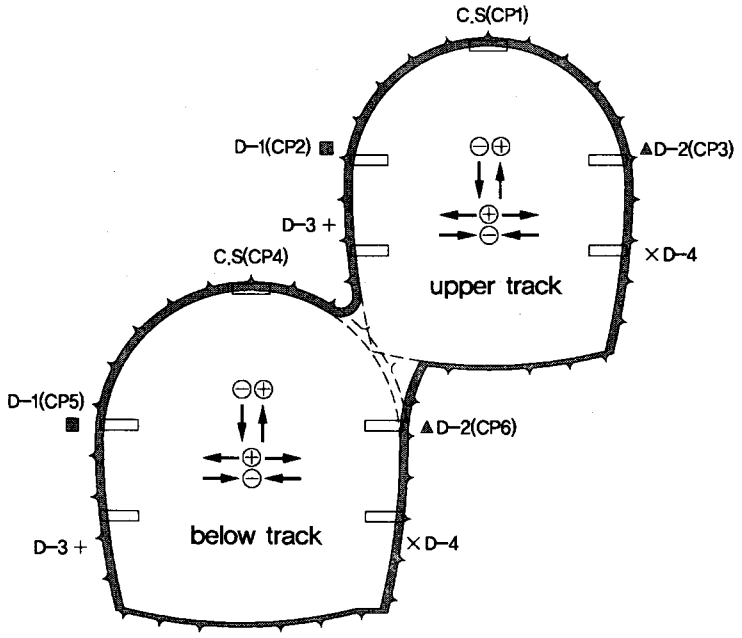

Fig. 5 five measurement points on each track in a cross section

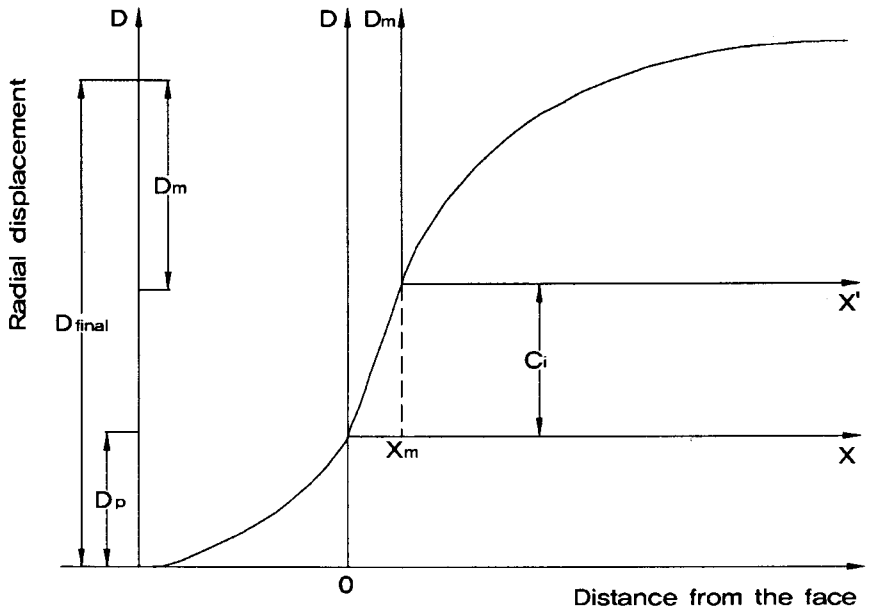

Fig. 6 Generalized form of tunnel convergence

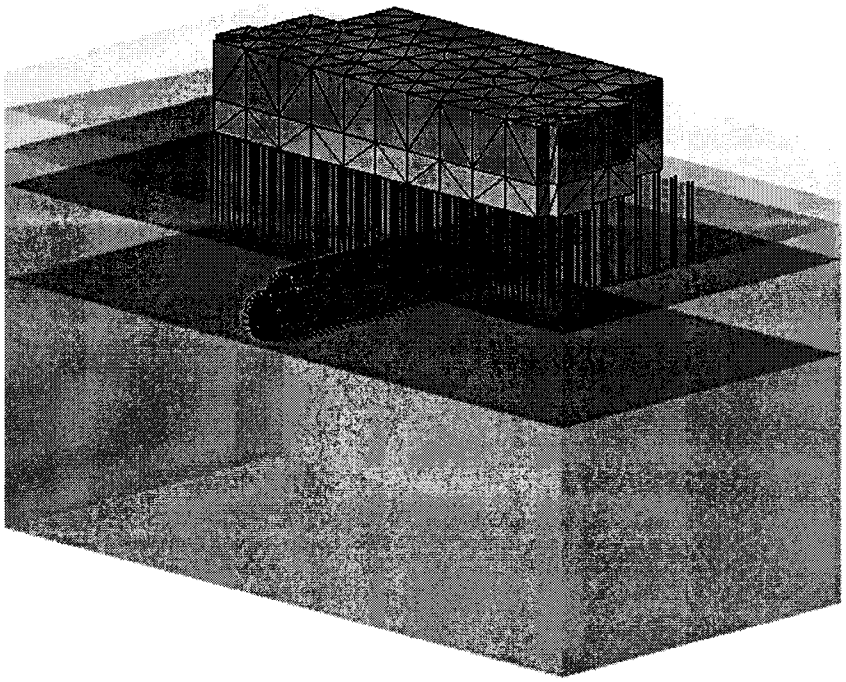

Fig.7 Three dimensional model boundary

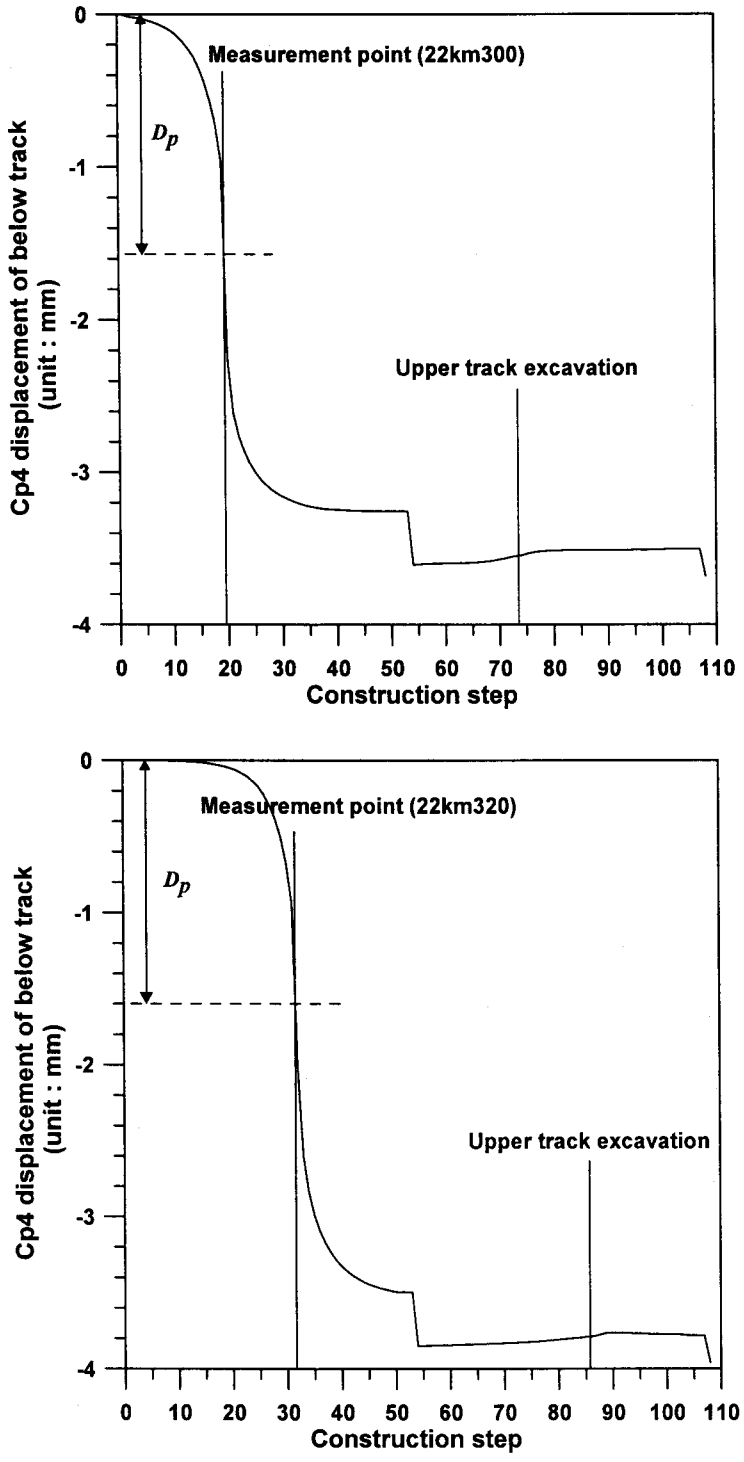

Fig. 8 Deformation behavior in Cp4 of below track at sta. 22km300 and 22km320

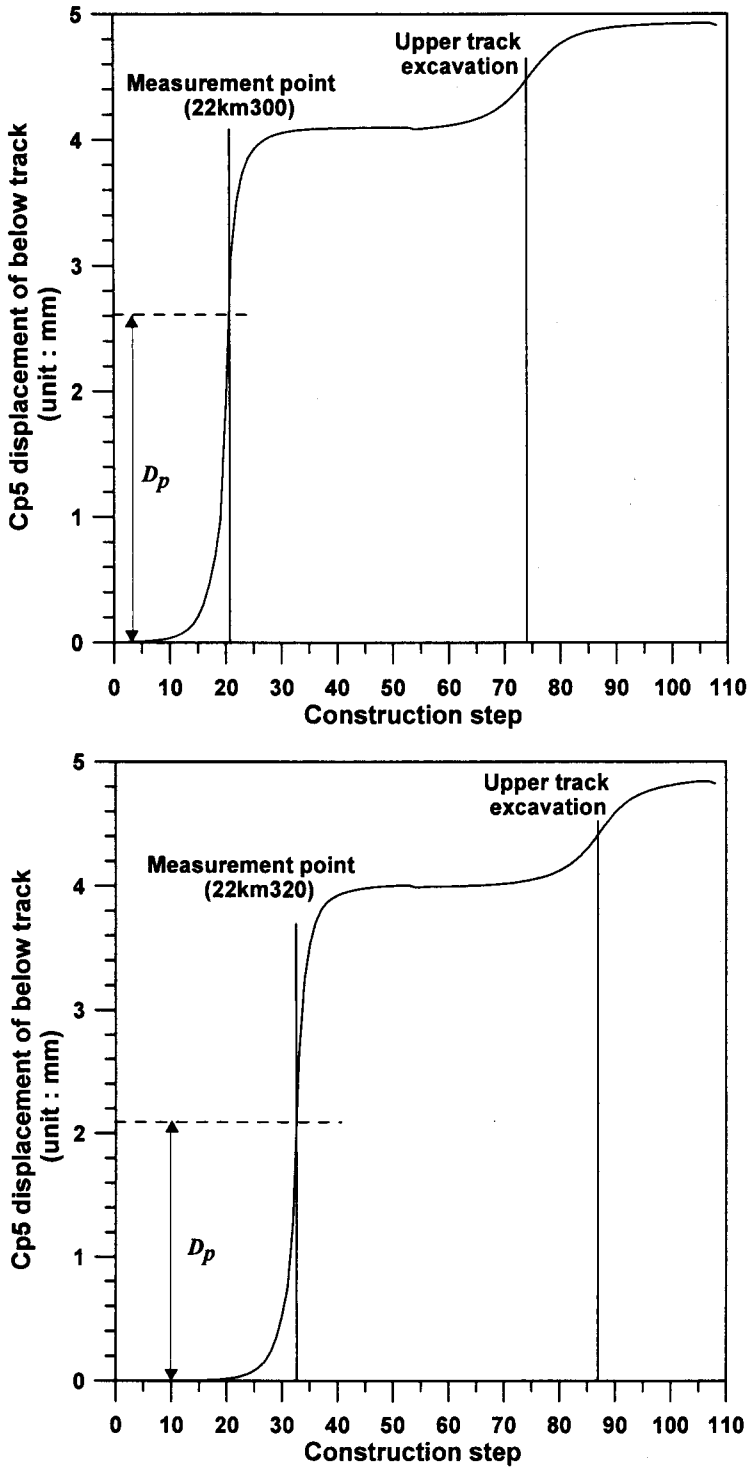

Fig. 9 Deformation behavior in Cp5 of below track at sta. 22km300 and 22km320

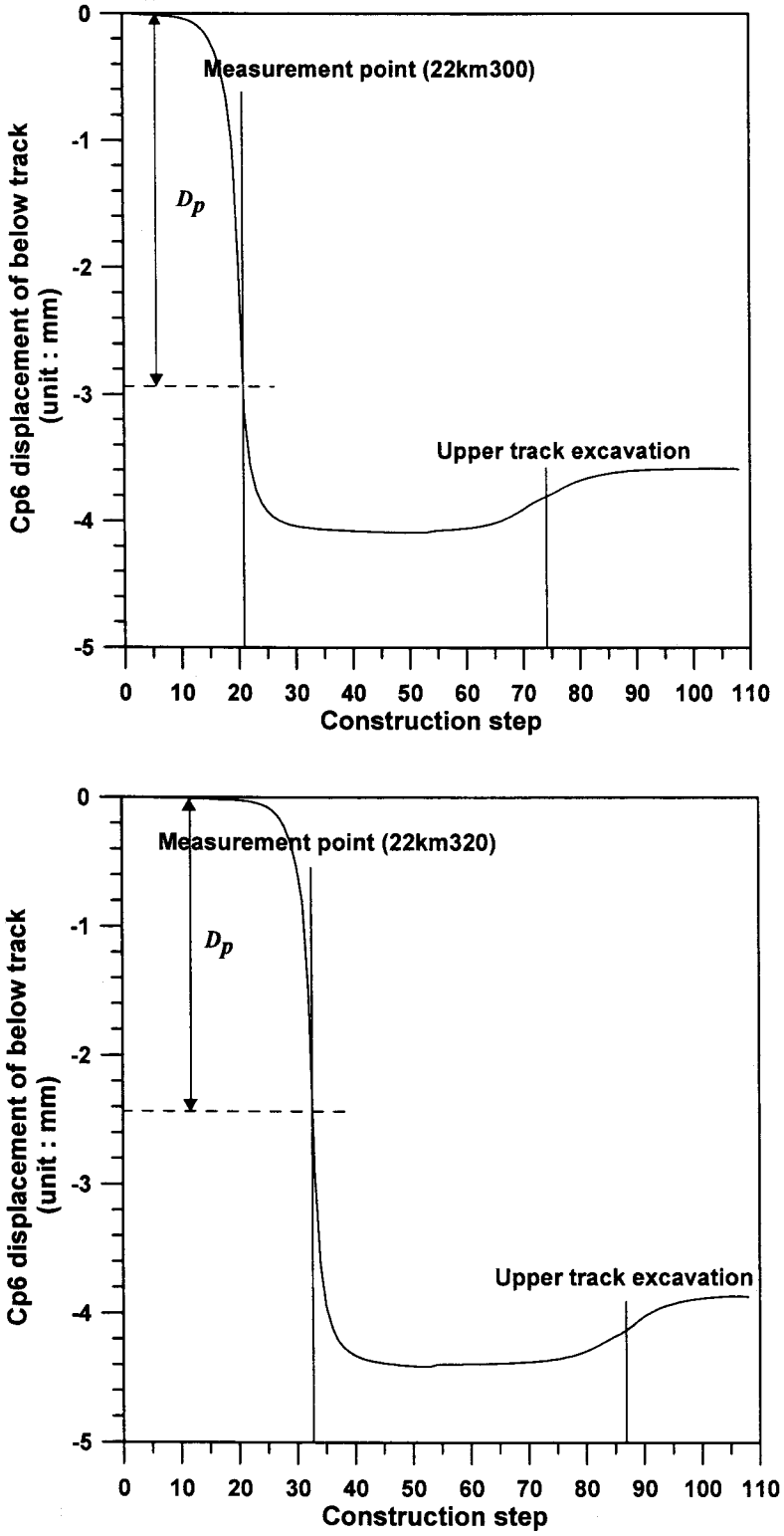

Fig. 10 Deformation behavior in Cp6 of below track at sta. 22km300 and 22km320

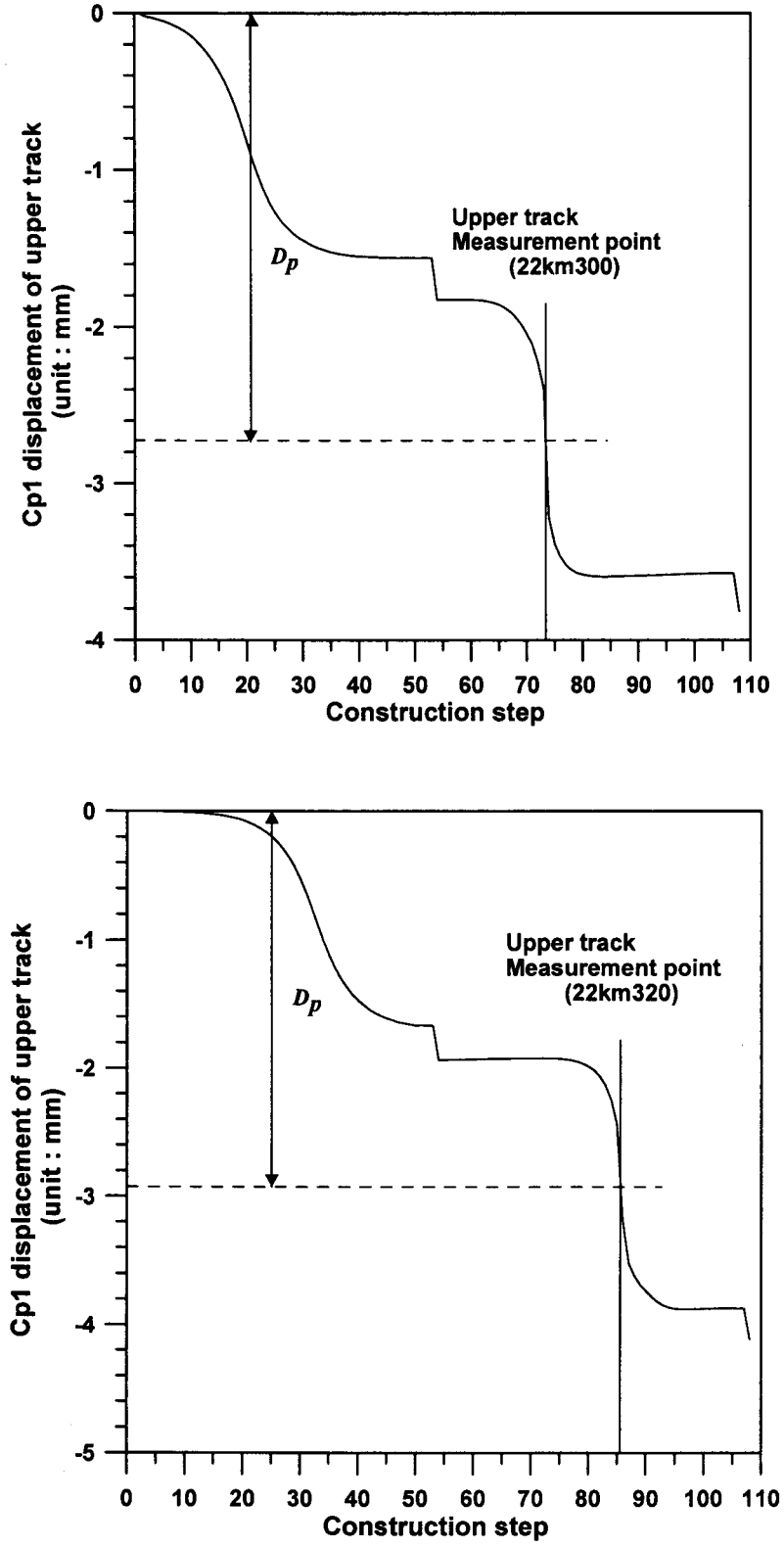

Fig. 11 Deformation behavior in Cp1 of upper track at sta. 22km300 and 22km320

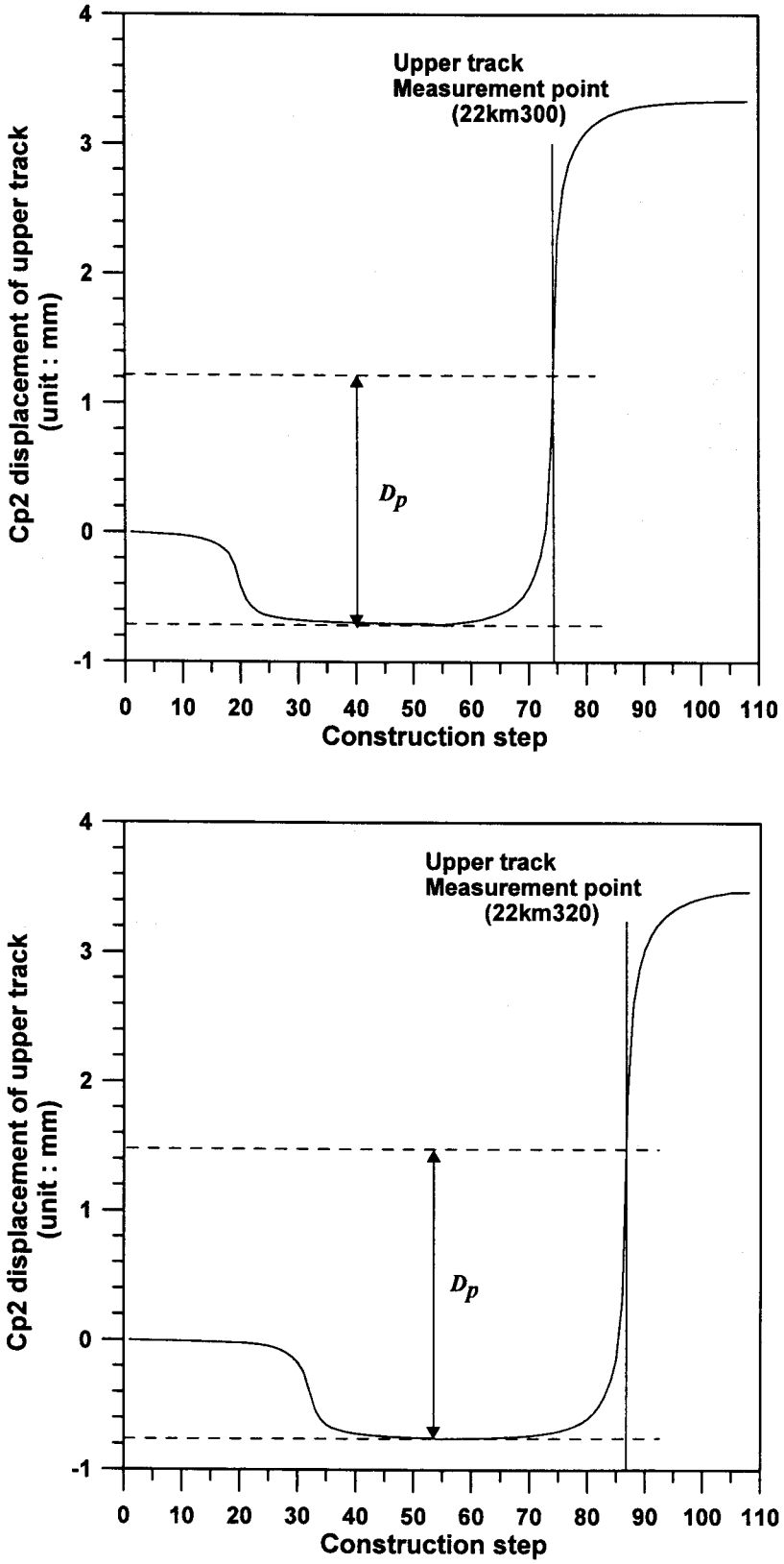

Fig. 12 Deformation behavior in Cp2 of upper track at sta. 22km300 and 22km320

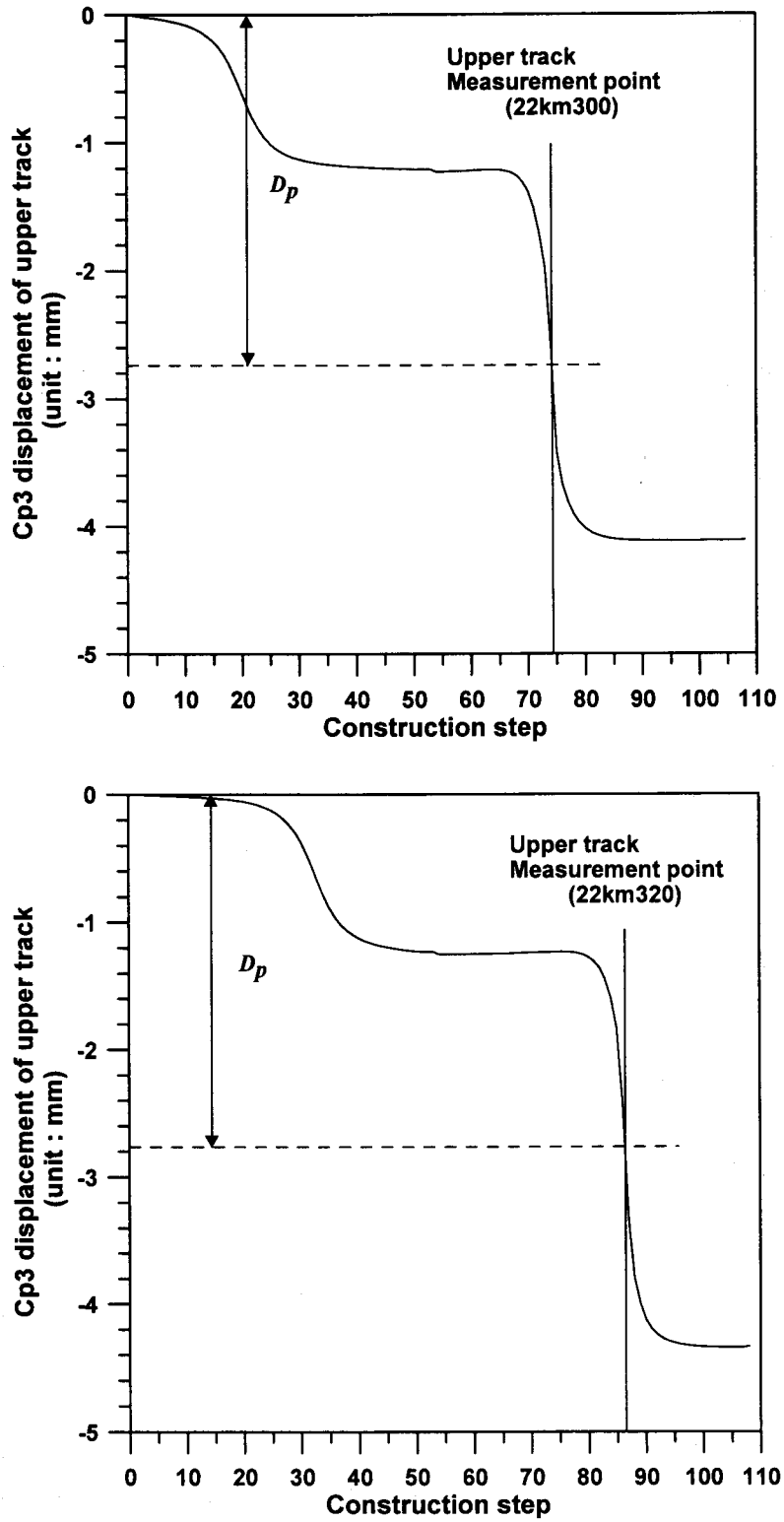

Fig. 13 Deformation behavior in Cp3 of upper track at sta. 22km300 and 22km320

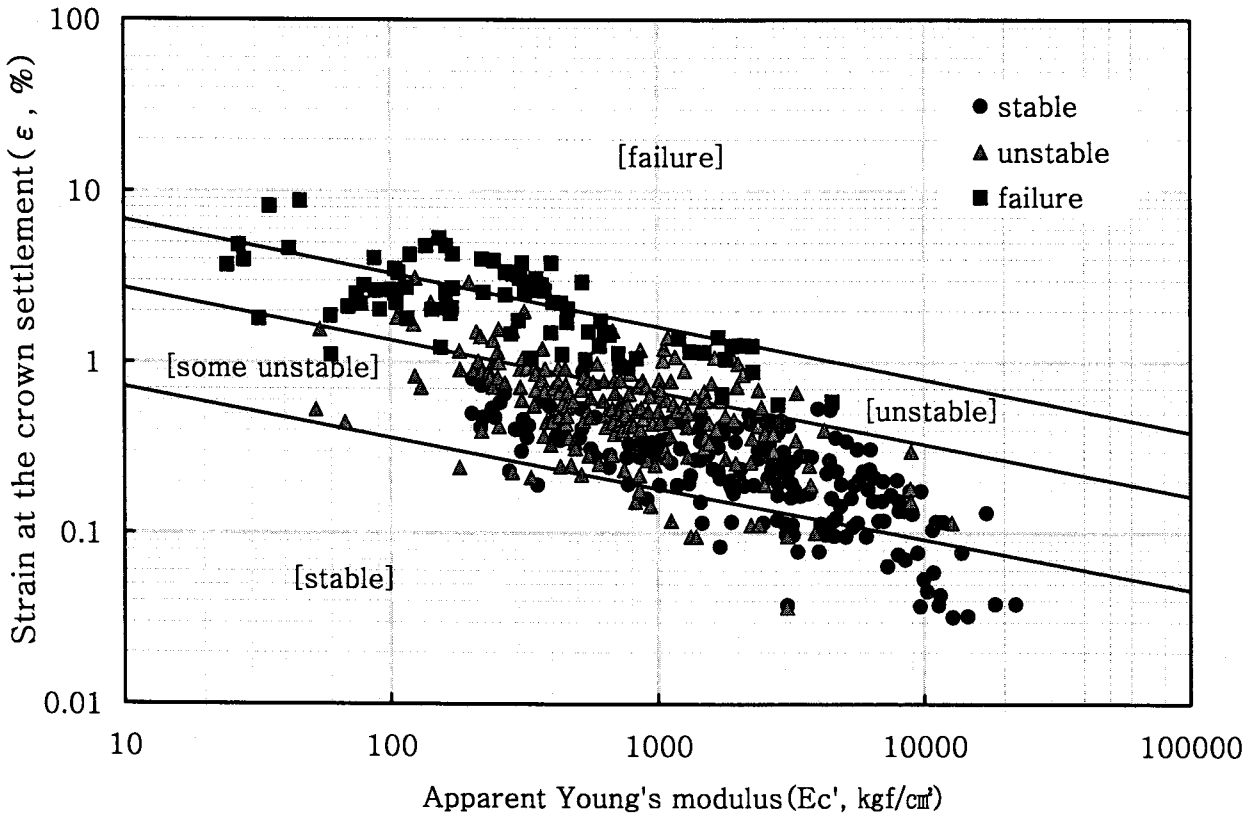

Fig. 14 Critical strain and apparent Young s modulus estimation

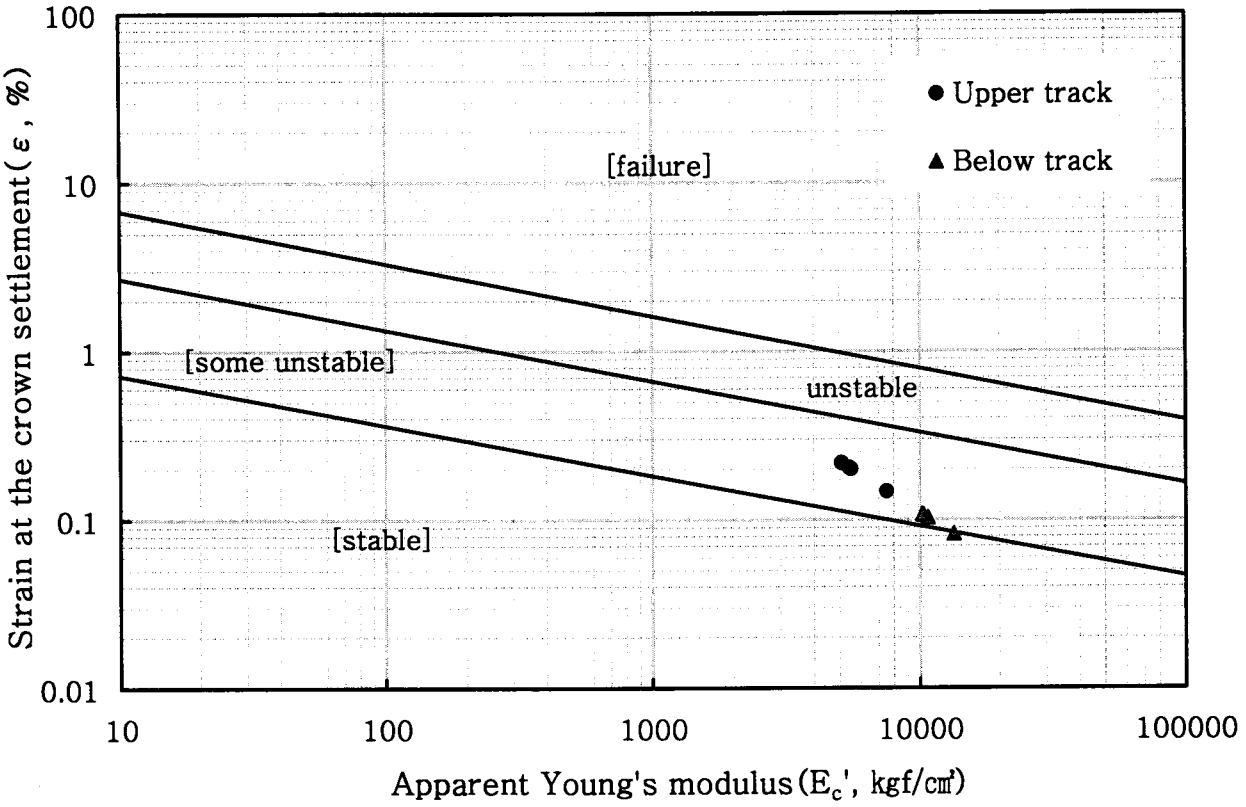

Fig. 15 Critical strain and apparent Young s modulus estimation about tunneling around the airport cargo